



Influence of welding parameters on material flow, mechanical property and intermetallic characterization of friction stir welded AA6063 to HCP copper dissimilar butt joint without offset

T. K. BHATTACHARYA, H. DAS, T. K. PAL

Welding Technology Centre, Metallurgical and Material Engineering Department,
Jadavpur University, Kolkata 700032, India

Received 3 September 2014; accepted 1 April 2015

Abstract: Joining of dissimilar aluminium–copper is an emerging area of interest for both research and industry due to its complex nature. Friction stir welding was attempted to evaluate the joint strength without offset at the butt line between AA6063 to HCP copper sheet under different combination of rotational speed of 800 and 1000 r/min and travel speed of 20 and 40 mm/min. Material flow was studied in detail for different combinations of parameters with optical microscopy and elemental mapping by energy dispersive X-ray spectroscopy (EDS). The results were correlated with the microstructural characteristics and formation of intermetallics at the bond interface using microhardness test and X-ray diffraction (XRD) technique. Material flow clearly suggests that energy input at 800 r/min and 20 mm/min is sufficient to plasticize both the materials with formation of higher amount of thermodynamically stable and hard intermetallic phases Al_4Cu_9 and $AlCu_4$ (slower cooling rate of 88 K/s) than that at 800 r/min and 40 mm/min (faster cooling rate of 154 K/s), attributed maximum joint strength (~78.6% of aluminium base metal).

Key words: friction stir welding (FSW); AA6063 alloy; HCP copper; material flow

1 Introduction

Nowadays, the joining of dissimilar materials is widely used in industrial applications due to their technical and beneficial advantages [1]. Aluminium (Al) and copper (Cu) are two most common engineering materials widely used in the aerospace, transportation and electric power industries [2–4]. Al/Cu dissimilar joint is of great interest because it maintains most of copper's specific properties and simultaneously it can reduce materials cost and mass while prolonging the service life in numerous industrial fields.

From practical point of views, sound joints between dissimilar materials with multi material design methodologies have to be established. Joining of dissimilar metals by conventional fusion welding techniques is difficult due to large differences in thermo physical properties like thermal conductivity, melting point, thermal expansion which leads to high distortion, residual stresses and also in metallurgical characteristics, resulting in the formation of brittle intermetallic phases

which are generally formed by solid state reaction. These intermetallics (IMC) generally result in mechanical degradation of the joint [1–6]. On the other hand, conventional solid-state welding methods like friction welding and ultrasonic welding have some limitations.

Friction stir welding (FSW) being a novel solid state joining process is envisaged to be a suitable alternative since it alleviates bulk melting of work pieces although initial investigations have indicated the presence of intermetallic compounds such as $AlCu$, Al_4Cu_9 and Cu_2Al in friction stir welded joints of aluminium to copper [1–6]. OUYANG et al [3] reported the poor weldability of aluminium and copper due to the formation of complex microstructure and various brittle IMCs in the nugget zone. XUE et al [4,7] studied the effect of process parameters such as tool offsetting, rotation rate and traverse speed on microstructure and mechanical properties of dissimilar 1060 aluminium–pure copper joints and reported that defect-free joints obtained good mechanical properties and excellent metallurgical bond. To improve the joint strength, an IMC layer seems to be necessary; but too thick IMC layer may initiate

crack and propagate easily through brittle IMC. A similar observation was reported by GALVÃO et al [8], LIU et al [9] and GENEVOIS et al [10]. Good mixing of Al and Cu, with large amount of fine dispersed Cu particles, was observed in the weld nugget zone and a composite-like structure formed, resulting in good tensile and bending strengths [2]. ESMAEILI et al [11] studied the feasibility of joining brass to 1050 aluminum alloy by friction stir welding process and reported that the tensile strength of the weld decreased with increase in rotation speed due to the disappearance of lamellar composite structure with thickening of interfacial intermetallic layer. Dissimilar joining of pure copper and 1350 aluminum alloy was studied by LI et al [6] and they observed that 1 mm to 2 mm pin offset on the aluminum side leads to sound joint and maximum ultimate tensile strength of around 160 MPa. ABDOLLAH-ZADEH et al [12] studied the effect of formation of hard and brittle intermetallic phase at the interface of the joints on the shear strength. From the above discussion, it is clear that metal flow around the tool is very complicated and that is why better understanding of the material flow is very much needed to improve process productivity and weld properties without pin offset.

The flow of material around the welding tool for Al–Cu dissimilar joints during friction stir welding (FSW) is a very key issue to determine the effect of microstructure and formation of intermetallics on mechanical properties of the joint. Friction coefficient will govern the contact condition as the friction between the shoulder and the work piece has the major contribution on the heat input and hence strongly affects the material flow. Strong deformation under the shoulder, strain and strain rate experienced by a material is directly related to the material's flow history. Visualisation of flow pattern in dissimilar joint is too complicated. Vertical flow as well as rotational flow of material around the pin is also important since the material is pushed down by the threads (for example, a right-hand thread turning counter clockwise). Reversing the direction of rotation of the pin (without changing the hand of the threads) generally results in an inferior weld [13]. NUNES et al [14] has emphasized the importance of the rotational flow of material around the nib. They have synthesized a model and reported that flow follows this path sequentially, firstly inward at the shoulder and then down at the nib threads after that outward on the lower part of the nib and finally upwards in the outer regions around the nib to complete the circulation. Complex, fluid-like flow patterns often arise as a result of irregular lamellae formed by the flow of one recrystallized regime within or over another.

However, a systematic study on the influence of the welding conditions and process response on the evolution of metal flow, thermal history with the formation of interfacial intermetallic compounds and deterioration of the weld joint properties is rare for aluminum to copper friction stir welded dissimilar joint.

The present work depicts a combined material flow and intermetallic characterization for dissimilar 6063 aluminium alloy to HCP copper joint by friction stir welding process without offset on the aluminium side. The nature and the extent of the intermetallic compounds across the weld joint interface are characterized by XRD and EDS mapping and correlated with the cooling rate derived from the thermal cycle. The consequent degradation of the weld joint mechanical properties is examined further for various welding conditions and correlated with the process response.

2 Experimental

Friction stir welding of 3.0 mm thick AA6063 and 3.0 mm thick electrolytic tough-pitch copper Cu-HCP (C-10300) sheet was performed in butt joint configuration with AA6063 placed at the retreating side and Cu-HCP placed at the advancing side using a RM series friction stir welder (Model RM1A-0.7). The machine can be operated with tool rotational speed up to 3000 r/min, axial load of 67 kN and plunge rates from 0.1 to 1000 mm/min. The axial force, torque and penetration depth values could be recorded simultaneously during each welding operation with the help of load cell coupled with a data acquisition system. FSW machine can be operated in two control modes, i.e., force control mode and displacement control mode. The depth of penetration in displacement control mode and force in force control mode were kept constant. In this study, all the butt welds were made under displacement control mode. *X* force, *Y* force, *Z* force and torque were recorded for each joint. The tool used was made of steel SKD61 and comprised of a shank, shoulder (20 mm in diameter) and conical probe. The tool was tilted by 2° with the vertical axis in the direction opposite to the welding speed. A dwell time of 3 s after the complete plunging of the tool pin is maintained for all the experiments.

Chemical compositions and the mechanical properties of the base materials are shown in Table 1. Table 2 provides the welding conditions (rotational speed and travel speed) used for the FSW experiments in the present work with respective energy input, process response (*Z* force and torque) and tensile strength.

The energy for FSW was calculated using Eq. (1) [15] and the energy values are summarized in Table 2.

Table 1 Chemical compositions and mechanical properties of AA6063 and Cu-HCP (C-0300) base material

Grade	Thickness/mm	Chemical composition/%				Mechanical property/MPa	
		Al	Si	Mg	Cr	YS	UTS
AA 6063	3	98.80	0.52	0.478	0.10	172	220
Cu-HCP	3	Cu	P	O	Fe	206	231
		99.982	0.0034	0.0044	0.0012		

Table 2 Process response, energy input and joint strengths for different combination of parameters

Rotational speed/(r·min ⁻¹)	Travel speed/(mm·min ⁻¹)	Z force/kN	Torque/(N·m)	UTS/MPa	Energy/kJ
800	20	8.3	25.4	173	255.7
1000	20	6.4	23.1	115	415.3
800	40	9.1	29.2	100	163.9
1000	40	7.3	24.5	150	285.2

$$E = \int_{t=0}^t C_z(t) \frac{2\pi N_p}{60} dt \quad (1)$$

where C_z and N_p respectively represent torque and rotational speed.

The online temperatures were measured at the middle portion of the total weld length using K-type thermocouples that were placed at a depth of 0.5 mm from the bottom of the copper surface and at a distance of 4 mm from the butt line (close to the stir zone). The weld joint tensile strength was evaluated using transverse subsize tensile specimens as per ASTM E8M–04 standard in a 100 kN universal testing machine (INSTRON 8862) at a cross head speed of 5 mm/min. Microhardness experiments done at the top, middle and bottom of the weld cross section at a distance of ~0.8 mm from the top of the weld along the tool traverse direction were carried out using a fully calibrated Lica Vickers microhardness tester (model: A-1170) at load 0.98 N and a dwell time of 30 s. Optical microscopy analysis was conducted using a Carl Zeiss made Axio Imager A1m microscope. The X-ray diffraction (XRD) analysis was carried out at slow scan rate of 0.5 (°)/min using a target of Cu K_α to identify the interfacial intermetallic compounds. Fracture surfaces of the tensile fractured specimens were examined under JEOL JSM–8360 scanning electron microscope (SEM) to understand the mode of fracture and energy dispersive X-ray spectroscopy (EDS) elemental mapping and point analyses have been made on the interface region with SEM in OXFORD instrument model No. 7582 using INCA software.

3 Result and discussion

3.1 Thermal cycle

Heat is generated due to the friction between the shoulder and the work piece in friction stir welding and

the understanding of the peak temperature arising with combination of parameters is very important. Thermal cycle and peak temperature measurement for a combination of parameters of friction stir welded dissimilar aluminium to copper butt joint are shown in Figs. 1(a) and (b). It is clearly observed that temperatures are higher and the thermal cycles are stronger with increasing rotational speed at both the travel speeds of 20 and 40 mm/min. This is due to the fact that with increasing rotational speed, more intense deformational heating consistent with the reduction in frictional heating is prevailed [16]. It is interesting to see from Fig. 1(c) that at 1000 r/min and travel speed of 20 mm/min, peak temperature is higher in aluminium side than that in copper side. It is quite obvious that the thermal coefficient of copper is higher than that of aluminium.

3.2 Force and torque responses

Analysis of the forces and torques which are transmitted to the FSW machine, is necessary to provide insights into the simultaneous process of thermally activated softening, strain and strain rate hardening and deformation that occur during FSW. Since torque is a measure of the shear stress and since shear stress on the work piece is responsible for heat generation [16]. Force and torque data during FSW may be considered to use as weld quality check. The axial force evolution is the work-piece material response of the applied process parameters [17]. Therefore, it is not unexpected that Z force will vary depending on conditions of material prevailing surrounding the tool. In fact, Z force will increase or decrease depending on flow resistance of the material. The rise and fall in Z force response for both 800 and 1000 r/min with respective two travel speeds 20 and 40 mm/min are quite obvious. Close look into the Figs. 2(a) and (b), the interesting thing is that the rise and fall in Z force response are in quite well manner. There is a large difference between the physical properties, thermal

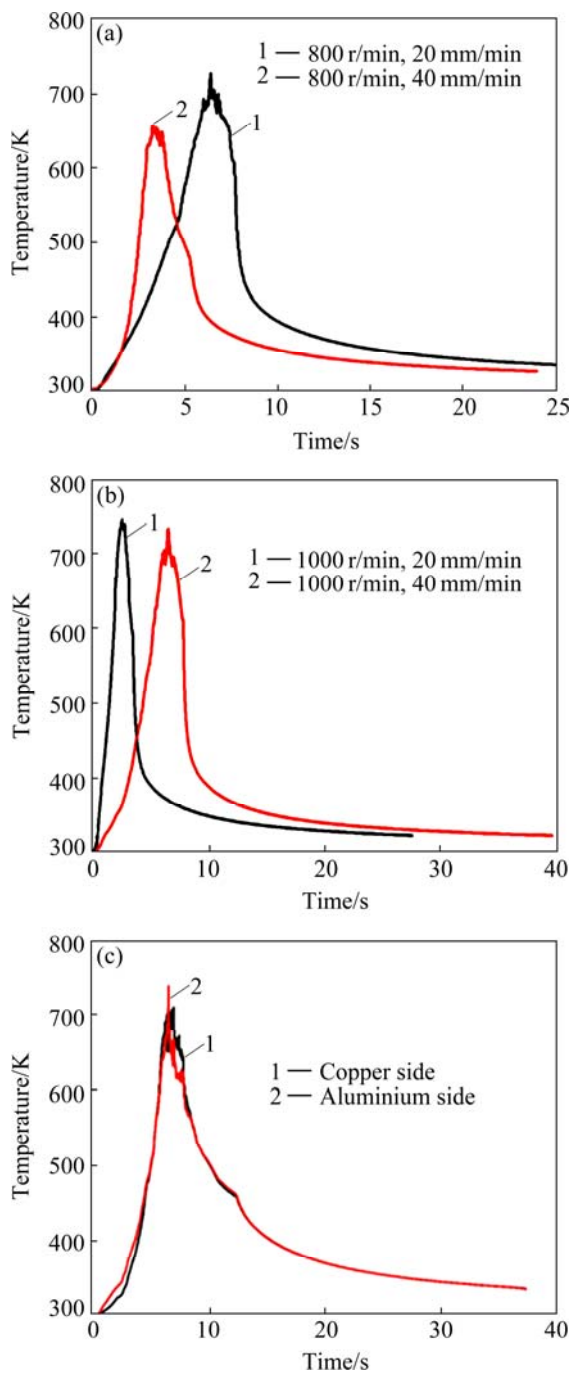


Fig. 1 Thermal cycle for 800 r/min (a) and 1000 r/min (b) at travel speeds of 20 mm/min and 40 mm/min and 1000 r/min and 20 mm/min at aluminium and copper side (c)

conductivity and melting point of the two materials. One part of the shoulder is in touch with comparatively softer aluminium in the retreating side and other part is in the cooper at the advancing side. As a result, shoulder experience different frictional force with two different materials at a single rotation. With rotation of the tool, retreating side aluminium tries to move towards the advancing side copper. That's why the fluctuation in the response curve is in a synchronized way.

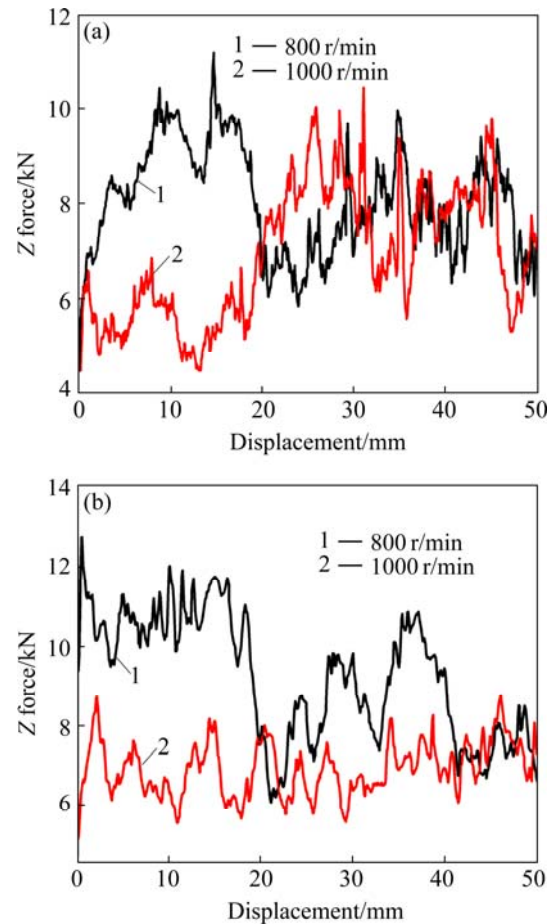


Fig. 2 Z force responses of 800 r/min and 1000 r/min at constant travel speed of 20 mm/min (a) and 40 mm/min (b)

It is clearly seen from Figs. 2(a) and (b) that at constant travel speeds of 20 and 40 mm/min, Z force decreases as the rotational speed increases from 800 to 1000 r/min. With increasing rotational speed, the deformation as well as frictional heat generation increases and hence, the material is thermally softened more quickly. Therefore, the welding process proceeds at lower load with increasing rotational speed.

It is observed that the torque increases with decrease in rotational speed (Figs. 3(a) and (b)) due to the modification of material flow around the tool changing the material viscous characteristics [17]. The stirring generates material plastic deformation around the pin, increasing the rotational resistance and consequently, the spindle torque. It can be observed from the Fig. 2 and Fig. 3 that the lowest axial force is associated with the lowest torque and the highest axial force is associated with the highest torque. This is due to the generated thermo-mechanical interactions between the tool and the work piece.

3.3 Material flow

Material flow of aluminium and copper dissimilar FSW joint at 800 r/min and 20 mm/min combination of

parameter shows several dark and bright areas of swirl and vortex flow patterns shown in Fig. 4. Recrystallized bulk copper is seen near the advancing side of the weld nugget, indicating intense deformation during FSW. A large volume mixing of both base materials in the weld nugget, is an indication of good amount of material extruded from the advancing side. Moreover, smooth

flow of retreating side material behind the tool pin is also clearly seen from Figs. 5(a) and (b). Mainly the lamellar or the swirl patterns are seen near the advancing side of the nugget, although the vortex flow is seen on the retreating side of the weld nugget (Fig. 6).

Various swirl and vortex flow patterns can be seen which is a clear indication of intense material mixing.

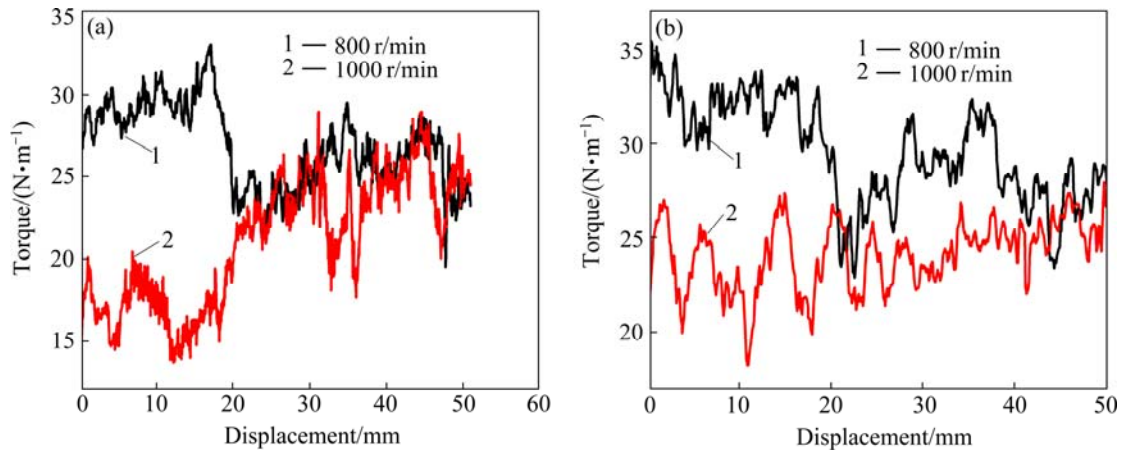


Fig. 3 Torque responses of 800 r/min and 1000 r/min at constant travel speed of 20 mm/min (a) and 40 mm/min (b)

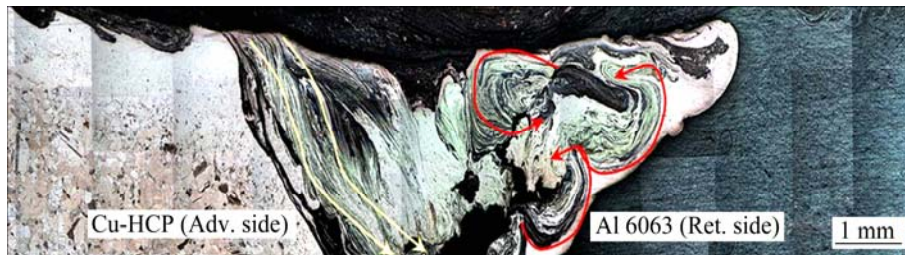


Fig. 4 Material flow in FS weld at 800 r/min and 20 mm/min combination of parameter

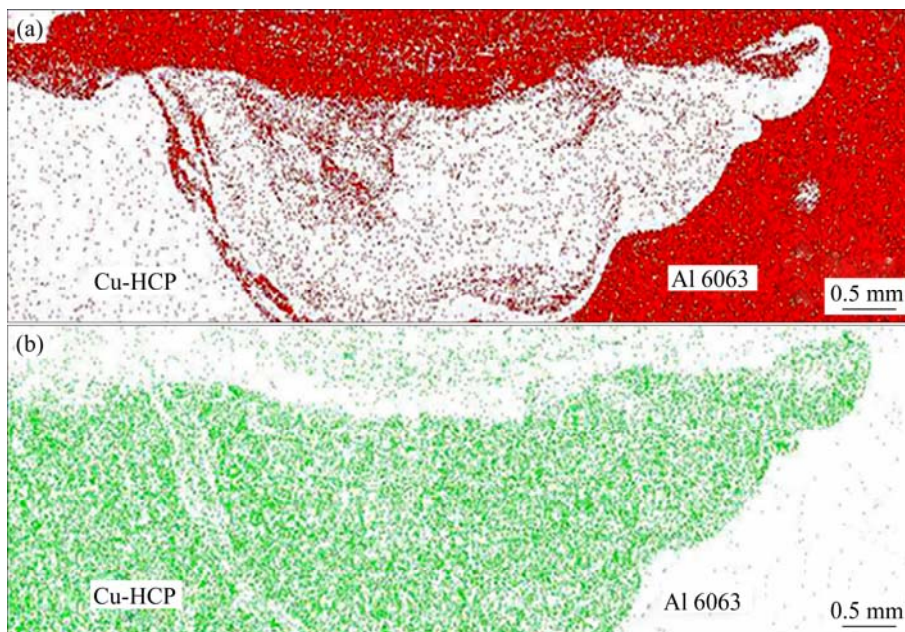


Fig. 5 Flow pattern by EDS elemental mapping for aluminium (a) and copper (b) sides at 800 r/min and 20 mm/min

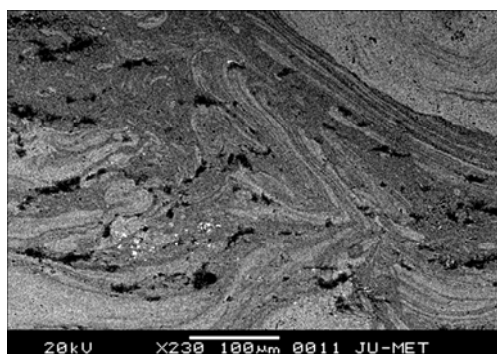


Fig. 6 Lamellar flow pattern

This shows the mixed material flows down the weld following streamline flow path shown by yellow lines in the macrostructure. Although under comparatively low heat input conditions, the HCP copper is sufficiently plasticized to mix with aluminium and flow down the pin, since in all of the welds, the heat input conditions are sufficient enough to plasticize the Al alloy. Moreover, the mixed material flows to the top middle part of the weld behind the pin and remains confined mostly on the retreating side of the weld nugget. High hardness values in top and middle parts of the weld of around HV 800 and HV 500 respectively show distribution of brittle intermetallics under the shoulder, which are identified from EDS mapping (Fig. 5). A large volume of mixed material zone having Al and fine Cu particles removes from the Cu base and some layered copper is seen under the shoulder influenced area in a large volume which is a clear indication that a large amount of retreating side material is pushed into the advancing side following the straight through current. Recrystallized bulk copper along the advancing side of the weld shows intense plastic deformation due to sufficient heat input conditions around the tool pin. This material flow clearly suggests that energy input at 800 r/min and 20 mm/min is sufficient to plasticize both the materials, resulting in sound weld joint with good joint strength.

At higher rotational speed of 1000 r/min and lower traverse speed of 20 mm/min, large amount of bulk copper is mixed with aluminium followed the conventional FSW flow model due to formation of adequate energy input (Fig. 7). Vertical movement of

mixed material in intercalated swirl patterns (lamellar flow) can be seen along the advancing side down the pin (shown by yellow lines). But no upward rotational flow of mixed material can be seen along the retreating side of the weld. The bulk copper extruded from the advancing side moving towards the upper layer of the mixed material zone is basically shoulder influenced deformed copper due to the effect of rotating threads (shown by red line). Due to very higher energy input (around 415 kJ), sticking condition is more predominating. As a result, the bulk copper sticks to the tool shoulder and is dragged by the threads in the shear layers where already retreating side aluminium flows towards the advancing side at the top of the weld. The right hand thread turning counter clock wise direction will drag the advancing side Cu down the threads of the pin following the maelstrom current. While the retreating side Al will be pushed to the advancing side following the straight through current. This process continues and under the action of threads, the mixed material flows down the pin when the shoulder surface touches the work piece. Bulk copper mixes with aluminium and the mixed material flows down the pin to the bottom of the weld in swirl like patterns along the advancing side of the weld. Some intermixed zone does not flow down and remains at the top of the nugget under the shoulder.

Material flow for 800 r/min and 40 mm/min combination of parameter is shown in Fig. 8. Peak temperature of 650 K in the copper side and a subsequent low energy input of 163.9 kJ are not sufficient enough to plasticize a good volume of bulk copper. For this reason, the copper dragged from the base material remains mainly in bulk form as it tries to mix with aluminium. Very small intermixed zone and lamellar flow patterns can be seen under the shoulder and near the tool pin nib.

It is clear from Figs. 9(a) and (b) that the flow fields are mainly confined in the top and lower parts of the weld. Due to lower heat input, bulk copper dragged from the base material does not flow downward to the pin, rather remains confined in the top/middle part of the weld nugget. A long range high hardness values distributed over the top of the weld nugget clearly indicate the formation of brittle aluminium copper intermetallics surrounded by bulk copper. While in the

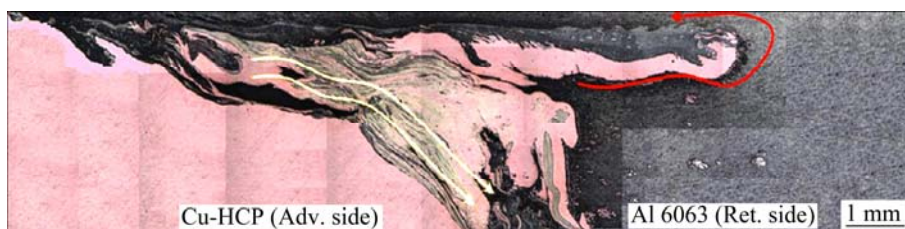


Fig. 7 Material flow in combination of parameters of 1000 r/min (CCW) and 20 mm/min

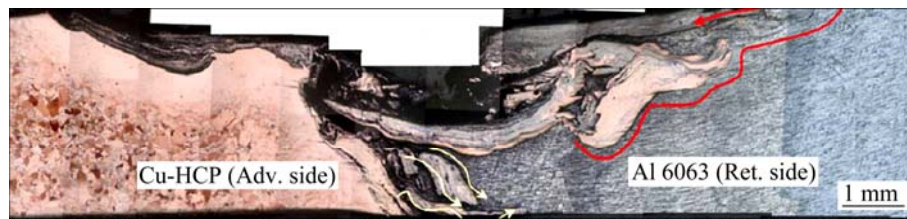


Fig. 8 Material flow in combination of parameters 800 r/min (CCW) and 40 mm/min traverse speed

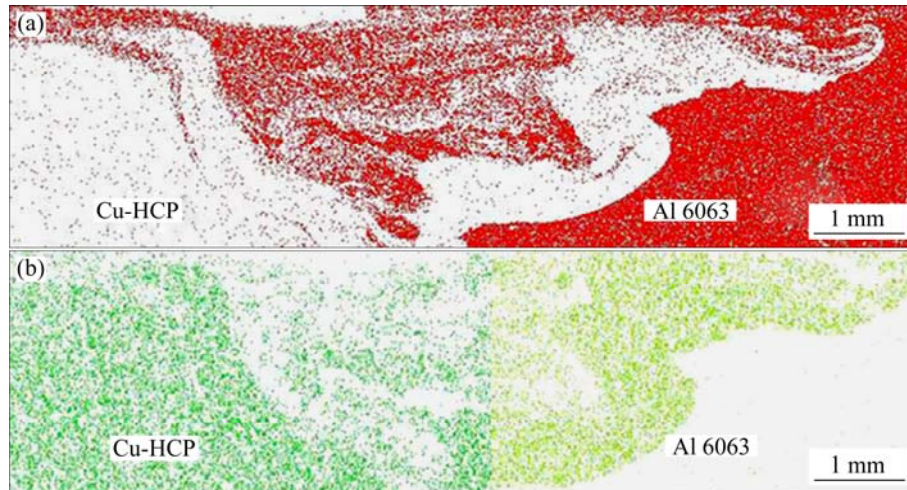


Fig. 9 Flow patterns by EDS elemental mapping for aluminium (a) and copper (b) sides at 800 r/min and 40 mm/min

middle bottom of the weld, streamline shaped mixed material flow is observed around the advancing side. Lamellar flow (Fig. 10) of mixed material trying to flow up around the tool pin nib can also be seen in the microstructure.

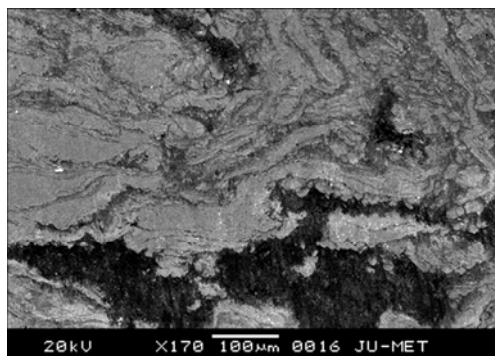


Fig. 10 Lamellar flow pattern for 800 r/min and 40 mm/min

Maximum hardness of around HV 250 is recorded in those areas for 800 r/min and 40 mm/min (Fig. 11). From Table 2, it is seen that average torque (29.2 N·m) and average Z force (9.1 kN) values are quite higher than those of other parameter combinations. It is a clear indication of less plasticization of the material, sliding condition predominates. That is why the tool just passes the plasticized aluminium, without dragging sufficient aluminium from the retreating side behind the pin under

the shoulder area. Also, the bulk copper on the top of the weld provides hindrance to the flow of aluminium.

A large material mixed zone (Fig. 12) can be seen in the weld nugget with an irregular and heterogeneous material flow for combination of parameters of 1000 r/min and 40 mm/min. It can be seen that the mixed material has tried to flow to the top of the weld as shown by the white arrow. Intermixed streamline shape Al–Cu layered structure can be seen on the retreating side of the weld (golden yellow and black/silverfish layers) as well as on the advancing side in small amount. Copper layers can be seen in the weld nugget in elongated shape. It is seen that along with larger amount of bulk copper removed from base material, sufficient volume of aluminium is also pushed from the retreating side to the advancing side of the weld.

Due to higher rotation rate, large volume of bulk copper is removed from the Cu base metal and is mixed with aluminium which is pushed from retreating side to the advancing side of the weld. So, a greater mixed material zone is observed in the weld nugget. As seen in most of the other FS welds here, the mixed material zone is mainly confined on the shear surfaces of the tool pin and under the shoulder influenced area. Though the mixed material has tried to flow to the top of the weld but higher traverse speed fails to do so and gets heterogeneously distributed in the weld nugget. Several

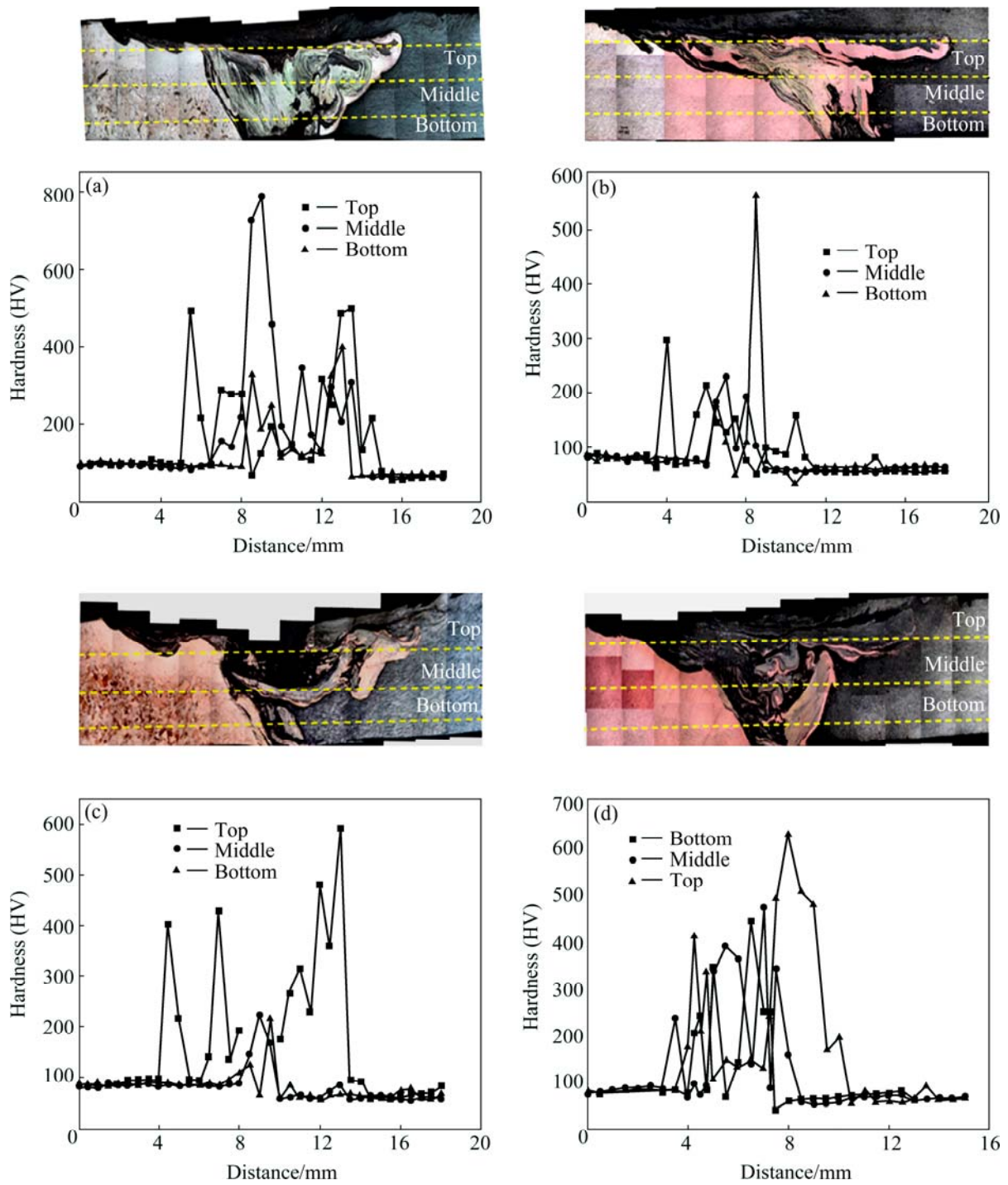


Fig. 11 Hardness distribution at top, middle and bottom of welded joint performed at 800 r/min and 20 mm/min (a), 1000 r/min and 20 mm/min (b), 800 r/min and 40 mm/min (c), 1000 r/min and 40 mm/min (d)

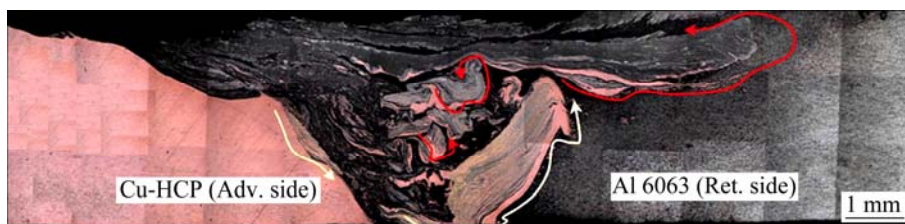


Fig. 12 Material flow in FS weld at 1000 r/min (CCW) and 40 mm/min traverse speed

streamline or lamellar structures can be seen in the nugget which reveals different colours on etching. The golden yellow region with high hardness of around HV 650 and the black silverish region with hardness of around HV 300–400 are copper and aluminium rich intermixed lamellae, respectively. Elongated copper on the top of the weld shows obvious plastic deformation of the bulk Cu under the action of the shoulder. Due to moderate heat input conditions, several plasticized copper layers are extruded and mechanically mixed with aluminium in the advancing side of the weld. Both the materials are sufficiently plasticized to flow down the pin and move up.

3.4 Microhardness

From the microhardness data in Fig. 11 (discontinuity in Fig. 11(c) due to the voids), it is seen that high hardness values over a long range are achieved at the top of the weld nugget for all the four cases. It is a clear indication that a large intermixed zone is formed in the shoulder influenced area. Moreover, very high hardness values of HV ~ 750 shown in the case of 800 r/min and 20 mm/min combination of parameter indicate the formation of brittle intermetallic compounds in those areas.

Hardness is an indication of tensile strength. Accordingly, parameter combination of 800 r/min and 20 mm/min (HV ~ 450) shows maximum joint strength whereas combination of 800 r/min and 40 mm/min shows poor joint strength with average hardness of HV ~ 250 .

3.5 Correlation between weld pitch, energy and corresponding joint strength

At a constant travel speed of 20 mm/min, with increasing rotational speed from 800 to 1000 r/min, energy input increases from 255.7 to 415.3 kJ, the Z force decreases from 8.3 to 6.4 kN and torque decreases from 25.4 to 23.1 N·m.

At a constant travel speed of 40 mm/min, with increasing rotational speed from 800 to 1000 r/min, energy input increases from 163.9 to 285.2 kJ, the Z force decreases from 9.1 to 7.3 kN and torque decreases from 29.2 to 24.5 N·m.

It is interesting to note that the strength decreases when rotational speed increases from 800 to 1000 r/min at a given traverse speed of 20 mm/min and strength increases slightly when rotational speed increases from 800 to 1000 r/min at a given traverse speed of 40 mm/min. This variation of strength with rotational speeds for given traverse speed appears to be linked to the energy input of the welds. Since increasing rotational

speed results in increasing heat generation (energy) and increasing traverse speed decreases heat generation, it is appropriate to use combined effect of rotational speed and traverse speed as measure of heat generation. Energy input vs welding speed and rotational speed in the form of weld pitch has been plotted as shown in Fig. 13, which reveals the effect of two parameters on energy input and variation of strength with energy input. Very high energy input (~ 415.3 kJ) attributes poor joint strength (~ 115 MPa) and very low energy input (~ 154 kJ) also shows poor joint strength (~ 100 MPa). Better joint strength as marked in Fig. 13 was achieved only within a certain range of energy input (255 to 285 kJ). These show that energy has a significant effect on the microstructure and joint strength of 6063 aluminium alloy to copper dissimilar butt joint.

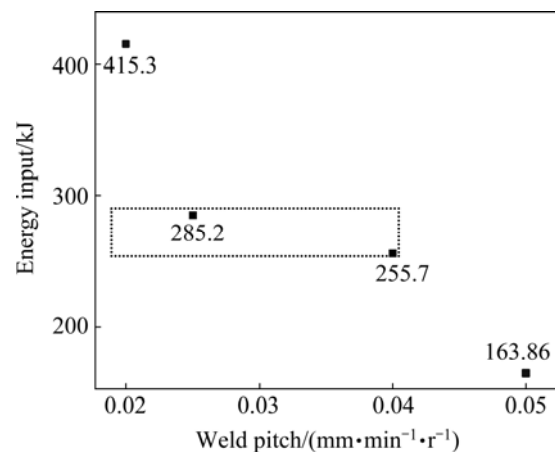


Fig. 13 Correlation between weld pitch and energy input

The interesting thing is that, the maximum torque and force are seen in the case of 800 r/min and 40 mm/min. Aluminum is more or less plasticized with that much of energy input, but copper is not properly plasticized at all. As a result, the torque is in higher side. Sliding condition is more prominent here and the advancing side copper cannot move smoothly towards the upper direction properly. The sliding torque represents the resistance of the less plasticized material against flow around the tool. An optimum amount of material flow around the tool with minimum resistance is needed for a good weld in FSW. Due to rubbing action of the pin, few copper particles inserted into the aluminium side rather than the formation of clear intermixing zone.

Furthermore, in the case of 1000 r/min and 20 mm/min, both the Z force and torque are around 2.7 kN and 6.1 N·m, respectively, which are less than those of 800 r/min and 40 mm/min. With very high energy input, both the materials are plasticized and sticking condition is more predominate here. However,

in the case of 800 r/min and 20 mm/min combination of parameter follows classical FSW flow model. Retreating side aluminum flows towards the advancing side copper as well as copper first moves towards downward and finally flows in the upward direction resulting sound weld joint without any defects.

3.6 XRD analysis of interface region

XRD analysis has been done for 800 r/min and 20 mm/min (highest joint strength) and 800 r/min and 40 mm/min (lowest joint strength). XRD results show that Al_4Cu_9 , Al_2Cu , AlCu_4 and AlCu are formed in both cases, and the results are shown in Fig. 14. Qualitative volume fraction is calculated from the XRD and the results are shown in Table 3.

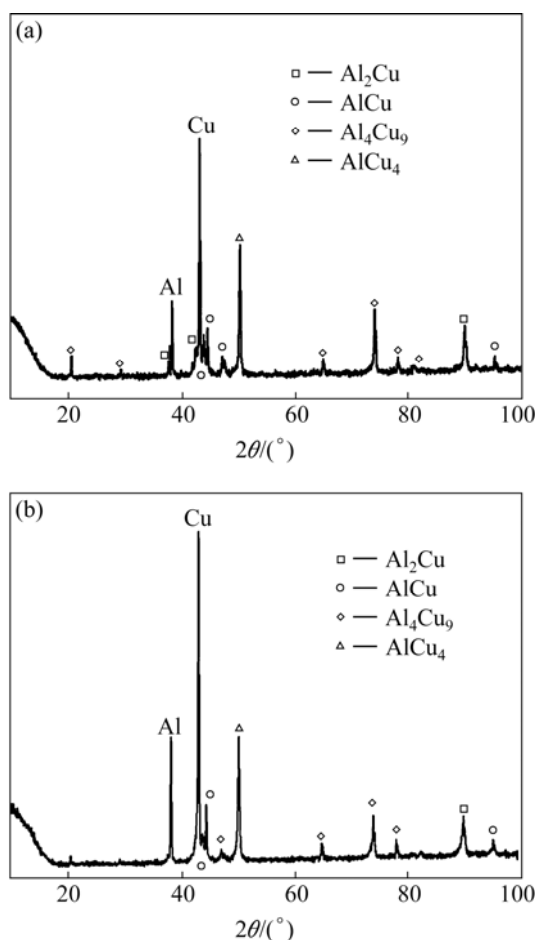


Fig. 14 XRD pattern for FS weld joints produced at 800 r/min and 20 mm/min (a), and 800 r/min and 40 mm/min (b)

Table 3 Volume fraction (%) of different intermetallic compounds for two different parameters

Parameter	Al_4Cu_9	Al_2Cu	AlCu_4	AlCu	Al	Cu
800 r/min and 20 mm/min	19.04	11.09	15.46	13.14	10.2	30.99
800 r/min and 40 mm/min	11.83	4.88	14.43	10.56	17.2	41.04

The interesting thing is that, Al_4Cu_9 , Al_2Cu and AlCu_4 are formed in higher amount in the case of 800 r/min and 20 mm/min than those at 800 r/min and 40 mm/min, as shown in Table 3.

From Table 4, it is seen that formation energy for Al_4Cu_9 is higher than that of AlCu and Al_2Cu . CHEN et al [18] stated that the solubility limit of Cu in Al is an order of magnitude less than that of Al in Cu, the $\text{Al}(\text{Cu})$ solid solution would be expected to saturate fast, resulting in the preferred nucleation of Al_2Cu . The formation of Al_2Cu requires more than double amount of Al needed for the formation of AlCu and more than 4 times the Al needed for Al_4Cu_9 for the same amount of consumed Cu.

Table 4 Formation energy for different intermetallic compounds

Phase	Formation energy, $\Delta H_f/(\text{kJ}\cdot\text{mol}^{-1})$
Al_2Cu	-13.05
Al_4Cu_9	-21.69
AlCu	-19.92

AlCu and Al_2Cu are basically metastable phase and kinetically favoured products. Peak temperature and energy input are quite higher at 800 r/min and 20 mm/min (728.6 K) than those at 800 r/min and 40 mm/min (652 K). It is well known that as the heat input is higher, cooling rate is slow. Due to slower cooling rate (88 K/s), thermodynamically stable Al_4Cu_9 and AlCu_4 form in higher amount in the case of 800 r/min and 20 mm/min. Whereas for 800 r/min and 40 mm/min, as the heat input is lower, cooling rate is fast (154 K/s), the Cu is not properly plasticized, and Al_4Cu_9 formed in a small volume fraction. Moreover, kinetically favoured AlCu is formed in higher amount than that at 800 r/min and 20 mm/min.

3.7 Fracture location and SEM fracture surface

In the case of 800 r/min and 20 mm/min, the fracture initiates from the top of the weld under the shoulder influenced area and travels along the stir zone and TMAZ boundary of copper, as shown in Fig. 15. Due to the presence of retreating side aluminium on the top of the weld, some ductility can be seen in Fig. 15(a). The area marked B shows quasi ductile-brittle mixed mode of failure, as can be seen from Fig. 16. Flat surface area with few dimples is a clear indication of such mixed mode of failure. Moreover, a long range mixed zone on the top of the weld with some copper particles and also higher hardness value indicating the development of brittleness with the presence of micro cracks can be the causes for the crack initiation in that area.

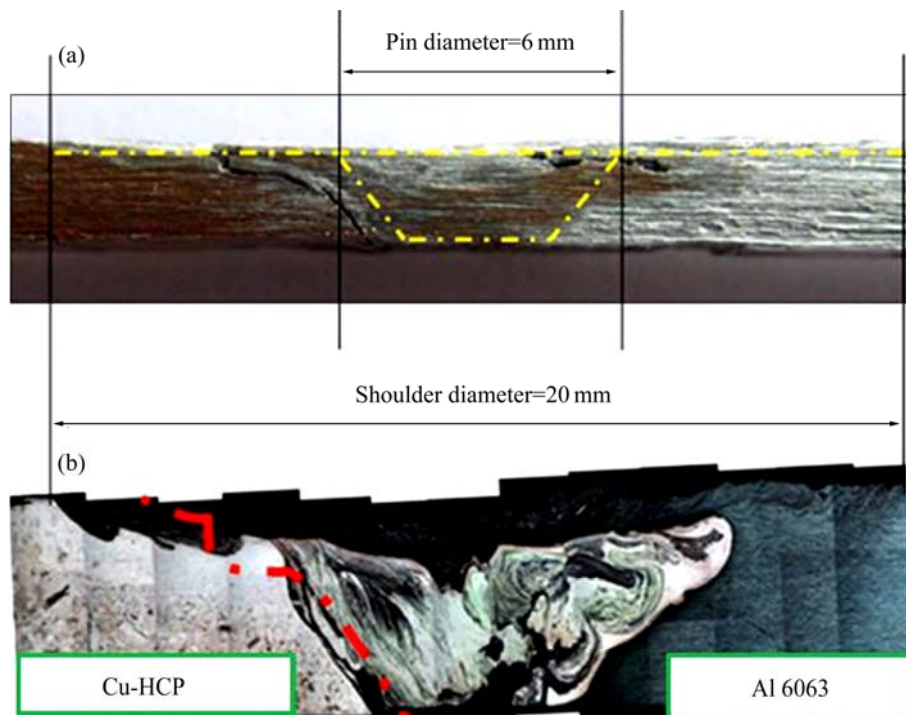


Fig. 15 Fracture location at tensile specimen (a) and marked by red line at macrostructure (b) for 800 r/min and 20 mm/min

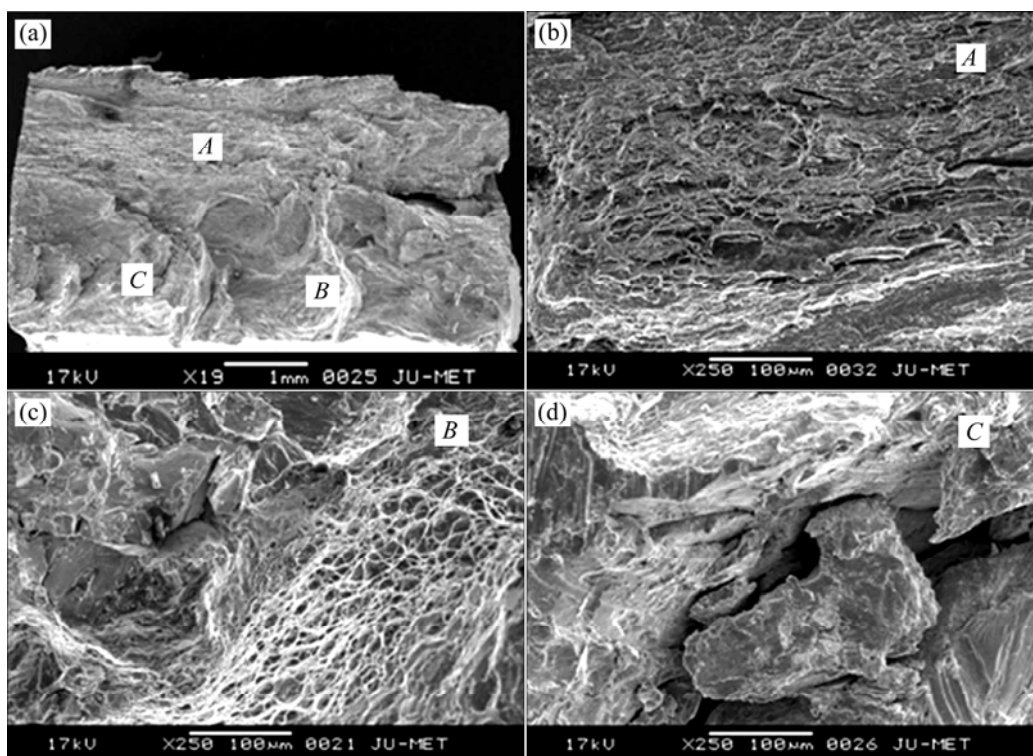


Fig. 16 Magnified view of fracture surface at different locations for 800 r/min and 20 mm/min

However, in the lower part of the weld in area *C*, presence of shear flat surface and tearing ridge features shows that extreme brittle fracture has occurred in those areas. In area *B*, a cleavage fracture formed at the crack can be seen.

For 800 r/min and 40 mm/min, the crack initiates from under the shoulder area as in the previous weld of 800 r/min and 20 mm/min and propagates along the stir zone. Finally, the tensile test specimen fails from weld nugget, as shown in Fig. 17.

Flat surface with the presence of a little ductility indicates that crack initiates from more brittle zone. A large intermixed region with higher hardness values in the upper part attributes to the crack initiation probability in that area. Obviously, the crack path follows towards

the weld nugget where void can be seen in the cross section of the weld (Fig. 17(a)). Large flat surfaces and micro-cracks are similar to tearing ridge features in Fig. 18(b) and river like patterns on the flat surfaces Fig. 18(c) clearly indicate cleavage fracture.

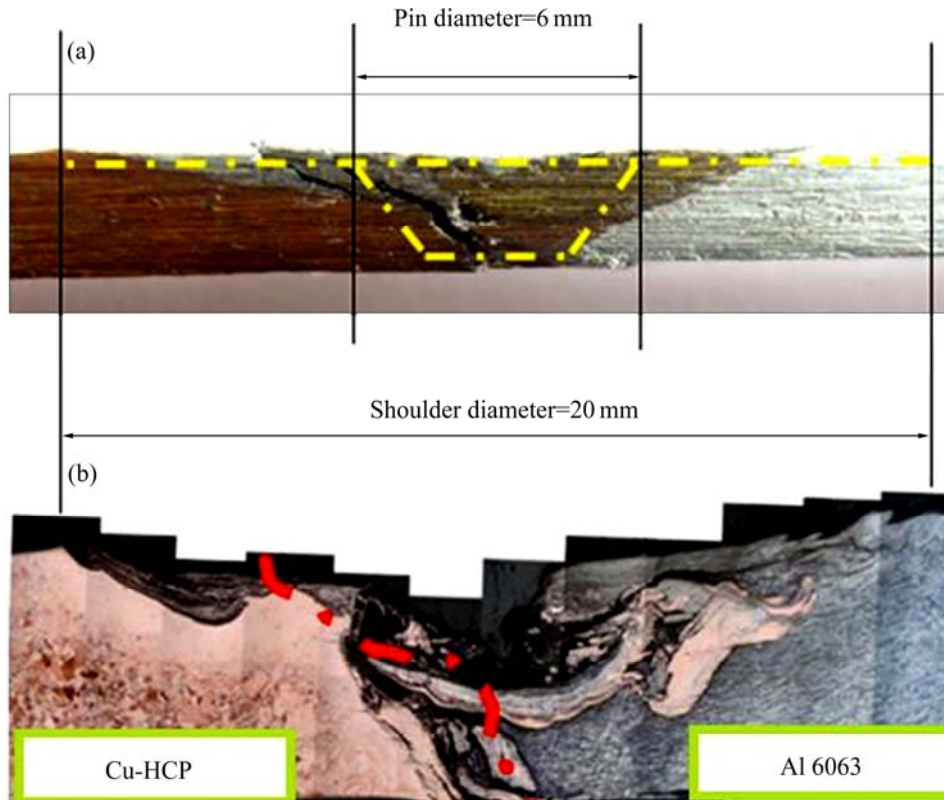


Fig. 17 Fracture location at tensile specimen (a) and marked by red line at macrostructure (b) for 800 r/min and 40 mm/min

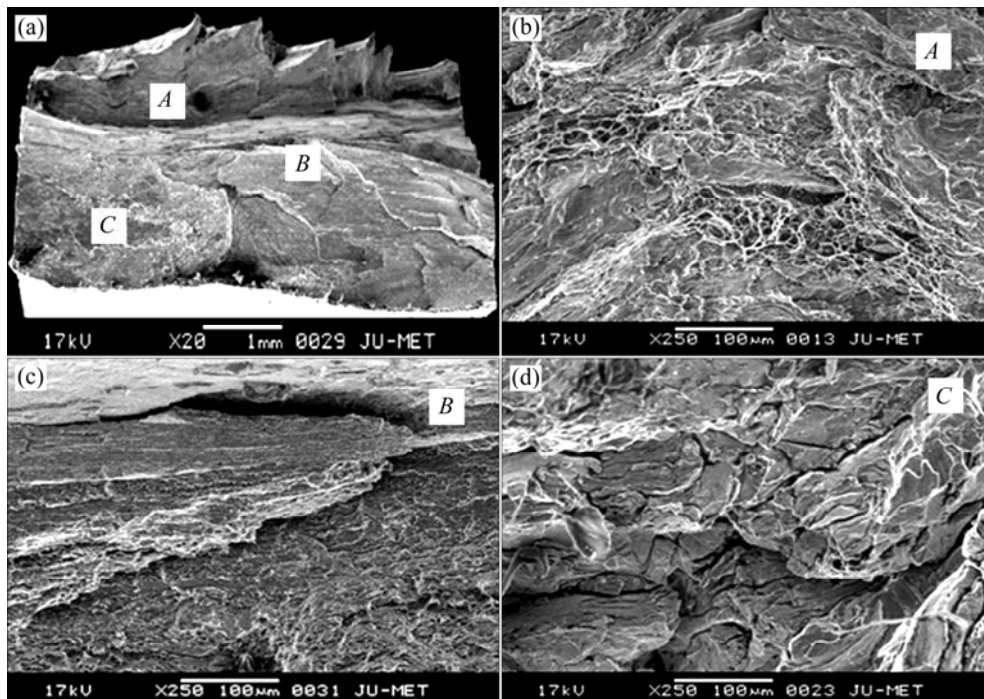


Fig. 18 Magnified view of fracture surface at different locations for 800 r/min and 40 mm/min

4 Conclusions

1) The butt joints of 6063 aluminium alloy and HCP copper were successfully made by FSW process without offset on the aluminium side. Maximum joint strength as high as ~78.6% of aluminium base metal has been achieved.

2) The average joint strength is significantly influenced by the thermal cycle and combined effect of rotational speed and travel speed as well as energy input. The optimized parameter 800 r/min and 20 mm/min with energy input and peak temperature contribute to high-performance joint.

3) Material flow clearly suggests that energy input in 800 r/min and 20 mm/min is sufficient to plasticize both the material resulted sound weld joint with good joint strength. But combination of parameter 800 r/min and 40 mm/min and 1000 r/min and 20 mm/min shows improper material flow due to sliding and sticking conditions, respectively.

4) The formation of thermodynamically stable and hard intermetallic phase Al_4Cu_9 and $AlCu_4$ at 800 r/min and 20 mm/min (slower cooling rate of 88 K/s) contributes to better joint strength than 800 r/min and 40 mm/min (faster cooling rate of 154 K/s).

Acknowledgement

The authors are very much thankful to Agrawal Metal Works Pvt. Ltd., Haryana for providing the HCP copper material.

References

- [1] SUN Z. Joining dissimilar material combinations: Materials and processes [J]. *Int J Mater Prod Technol*, 1995, 10: 16–26.
- [2] TAN C W, JIANG Z G, LI L Q, CHEN Y B, CHEN X Y. Microstructural evolution and mechanical properties of dissimilar Al–Cu joints produced by friction stir welding [J]. *Materials and Design*, 2013, 51: 466–473.
- [3] OUYANG J, YARRAPAREDDY E, KOVACEVIC R. Microstructural evolution in the friction stir welded 6061 aluminium alloy (T6-temper condition) to copper [J]. *J Mater Process Technology*, 2006, 172: 110–122.
- [4] XUE P, NI D R, WANG D, XIAO B L, MA Z Y. Effect of friction stir welding parameters on the microstructure and mechanical properties of the dissimilar Al–Cu joints [J]. *Materials Science and Engineering A*, 2011, 528: 4683–4689.
- [5] GALVAO I, LEAL R M, LOUREIRO A, RODRIGUES D M. Material flow in heterogeneous friction stir welding of aluminium and copper thin sheets [J]. *Science and Technology of Welding and Joining*, 2010, 15(8): 654–660.
- [6] LI X W, ZHANG D T, QUI C, ZHANG W. Microstructure and mechanical properties of dissimilar pure copper/1350 aluminium alloy butt joints by friction stir welding [J]. *Transactions of Nonferrous Metals Society of China*, 2012, 22: 1298–1306.
- [7] XUE P, XIAO B L, NI D R, MA Z Y. Enhanced mechanical properties of friction stir welded dissimilar Al–Cu joint by intermetallic compounds [J]. *Materials Science and Engineering A*, 2010, 527: 5723–27.
- [8] GALVAO I, OLIVEIRA J C, LOUREIRO A, RODRIGUES D M. Formation and distribution of brittle structures in friction stir welding of aluminium and copper: Influence of process parameters [J]. *Science and Technology of Welding and Joining*, 2011, 15(8): 681–689.
- [9] LIU P, SHI Q, WANG W, ZHANG Z. Microstructure and XRD analysis of friction stir welded joints for copper T2/aluminium 5A06 dissimilar materials [J]. *Materials Letters*, 2008, 62: 4106–4108.
- [10] GENEVOIS C, GIRARD M, HUNEAU B, SAUVAGE X, RACINEUX G. Interfacial reaction during friction stir welding of Al and Cu [J]. *Metallurgical and Material Transaction A*, 2011, 42(8): 2290–95.
- [11] ESMAEILI A, BESHARATIGIVI M K, RAJANI Z. A metallurgical and mechanical study on dissimilar friction stir welding of aluminium 1050 to brass (CuZn30) [J]. *Materials Science and Engineering A*, 2011, 528: 7093–7102.
- [12] ABDOLLAH-ZADEH A, SAEID T, SAZGARI B. Microstructural and mechanical properties of friction stir welded aluminium/copper lap joints [J]. *J Alloys and Compounds*, 2008, 460: 535–538.
- [13] GUERRA M, SCHMIDT C, MCCLURE J C, MURR L E, NUNES A C. Flow patterns during friction stir welding [J]. *Materials Characterization*, 2003, 49: 95–101.
- [14] NUNES A C, BERRISTEIN E L, MCCLURE J C. A rotating plug model for friction stir welding [C]// *Proceedings of the 81st American Society of Annual Convention*. Chicago. IL, 2000: 26–28.
- [15] ZIMMER S, LANGLOIS L, LAYE J, BIGOT R. Experimental Investigation of the influence of the FSW plunge process parameters on the maximum generated force and torque [J]. *International Journal of Advanced Manufacturing technology*, 2010, 47: 2011–2015.
- [16] AKINLABI E T, MADYIRA D M, AKINLABI S A. Effect of heat input on the electrical resistivity of dissimilar friction stir welded joints of aluminium and copper [C]// *Proceedings of the IEEE Africon*, 2011. The Falls Resort and Conference Centre, Livingstone, Zambia, 2011, 9: 13–15.
- [17] DAS H, BASAK S, DAS G AND PAL T K. Influence of energy induced from processing parameters on the mechanical properties of friction stir welded lap joint of aluminium to coated steel sheet [J]. *International Journal of Advanced Manufacturing Technology*, 2013, 64: 1653–1661.
- [18] CHEN C X, HWANG W S. Effect of annealing on the interfacial structure of aluminium-copper joints [J]. *Materials Transactions*, 2007, 40(1): 1938–1947.

焊接参数对非偏移异种焊接 6063 铝合金和 HCP 铜接头材料流动、力学性能及金属间化合物的影响

T. K. BHATTACHARYA, H. DAS, T. K. PAL

Welding Technology Centre, Metallurgical and Material Engineering Department,
Jadavpur University, Kolkata 700032, India

摘要: 由于其复杂的特性, 铝-铜异种焊接逐渐受到科学界和工业界的关注。在不同旋转速度(800 和 1000 r/min) 和行进速度(20 和 40 mm/min)组合条件下, 对 6063 铝合金与 HCP 铜板材进行非偏移搅拌摩擦焊接, 并对接头强度进行评价。采用扫描电镜和 EDS 元素分布研究不同参数组合下的材料流动。利用显微硬度测试和 X 射线衍射技术对显微组织和界面金属间化合物进行研究。材料流动分析表明, 与 800 r/min 和 40 mm/min(快冷却速度 154 K/s) 相比, 在 800 r/min 和 20 mm/min 条件下(低冷却速度 88 K/s), 能量输入足以塑化两种材料, 并形成热力学稳定的硬质金属间化合物 Al_4Cu_9 和 AlCu_4 , 得到最高的接头强度(78.6%铝基体强度)。

关键词: 搅拌摩擦焊; 6063 铝合金; 铜; 材料流动

(Edited by Yun-bin HE)